ACS APPLIED MATERIALS & INTERFACES

Research Article

www.acsami.org

Effective Bone Regeneration Using Thermosensitive Poly(*N*-Isopropylacrylamide) Grafted Gelatin as Injectable Carrier for Bone Mesenchymal Stem Cells

Zhiwei Ren,[†] Yang Wang,[†] Shiqing Ma,[‡] Shun Duan,[†] Xiaoping Yang,[†] Ping Gao,[‡] Xu Zhang,*[,‡] and Qing Cai*[,†]

[†]State Key Laboratory of Organic−Inorganic Composites, Beijing Laboratory of Biomedical Materials, Beijing University of Chemical Technology, 100029 Beijing, China

[‡]School and Hospital of Stomatology, Tianjin Medical University, 300070 Tianjin, China

Supporting Information

ABSTRACT: In this study, thermosensitive poly(*N*-isopropylacrylamide) (PNIPAAm) was grafted onto gelatin via atom transfer radical polymerization (ATRP). The chemical structure of PNIPAAm-grafted gelatin (Gel−PNIPAAm) was confirmed by XPS, ATR-IR, and ^{1}H NMR characterizations. Gel−PNIPAAm aqueous solution exhibited sol-to-gel transformation at physiological temperature, and was studied as injectable hydrogel for bone defect regeneration in a cranial model. The hydrogel was biocompatible and demonstrated the ability to enhance bone regeneration in comparison with the untreated group (control). With the incorporation of rat bone mesenchymal stem cells (BMSCs) into the hydrogel, the bone regeneration rate was further significantly enhanced. As indicated by micro-CT, histological (H&E and Masson) and immunohistochemical (osteocalcin and osteopontin) staining, newly formed woven bone tissue was clearly detected at 12 weeks postimplantation in the hydrogel/BMSCs treated group, showing indistinguishable boundary with surrounding host bone tissues. The results suggested that the thermosensitive Gel−PNIPAAm hydrogel was an excellent injectable delivery vehicle of BMSCs for in vivo bone defect regeneration.

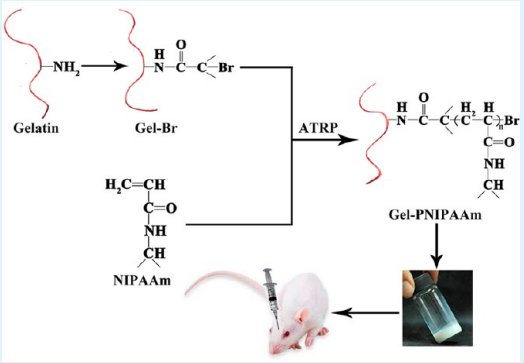

KEYWORDS: *thermosensitive, injectable, hydrogel, bone defect, bone mesenchymal stem cells*

INTRODUCTION

The integrity of bone is severely threatened by aging, disease, trauma and injury, etc. Regeneration of bone defects using concept of tissue engineering demonstrates promising approaches over conventional therapy using bone autograft or allograft.[1,2] For successful bone tissue regeneration to occur, the most common strategy is to fill bone defects with cell-scaffold constructs. The scaffold should provide an optimal three-dimensional (3D) environment, mimicking the natural extracellular matrix (ECM) of bone, for the attached cells to proliferate and differentiate.[3−5]

A variety of naturally- and synthetically derived materials have been formed into implantable scaffolds using methods as particle-leaching, phase separation, and 3D printing.[6−12] Compared to 3D scaffolds, the advantages of injectable materials are their adaption to irregularly shaped bone defects via minimally invasive surgeries.[13,14] Stimuli-responsive polymeric hydrogels are categorized as favorable substrates for bone regeneration, because they exhibit sol-to-gel transformation which is triggered by proper stimuli.[15] Various stimuli have been applied for preparing injectable hydrogels, including physical (thermal gelation, ionic interaction, self-assembly) and chemical (reactive agents, photopolymerization) cross-linking.[16−18] Among them, thermal gelation is easily handled and welcomed in clinical therapy. In particular, hydrogels formed by negative temperature-responsive phase transition have attracted intensive attention because the gelation occurs readily as the temperature being increased above the lower critical solution temperature (LCST), which is designed below body temperature.[19,20]

Natural biomaterials like collagen and chitosan exhibit excellent bioactivity due to their similar components to ECM. However, most of them do not have the feature of negative temperature-responsive phase transition. To endow them the thermo-sensitivity, incorporation of thermosensitive polymeric component onto the backbone of natural macromolecules is a commonly employed strategy. Poly(*N*-isopropylacrylamide) (PNIPAAm) is a typical example of thermosensitive polymers, which undergoes a coil-to-globule phase transition above its LCST (~32 °C).[21] It has been combined into various natural

Received: April 7, 2015
Accepted: August 12, 2015
Published: August 12, 2015

DOI: 10.1021/acsami.5b02821
ACS Appl. Mater. Interfaces 2015, 7, 19006−19015

polymers, such as chitosan,[22,23] collagen,[24] hyaluronic acid,[25,26] chondroitin sulfate,[27] and gelatin,[28] to form injectable hydrogels for cartilage and soft tissue regenerations. Therefore, combining thermosensitive PNIPAAm-modified biomacromolecular hydrogel with bone-related cells has a significant potential to treat orthopedic bone defects.

Generally, the grafting of PNIPAAm onto biomacromolecules involves steps of the synthesis of a carboxyl- or amino-terminated *N*-isopropylacrylamide (NIPAAm) prepolymer and the subsequent coupling reaction by using agents like carbodiimide.[29,30] In this study, atom transfer radical polymerization (ATRP) was employed to conduct the grafting of PNIPAAm onto gelatin backbone. By a bromination reaction, ATRP initiator (gelatin bromide, Gel−Br) was prepared and used to initiate the polymerization of NIPPAm (Figure 1).

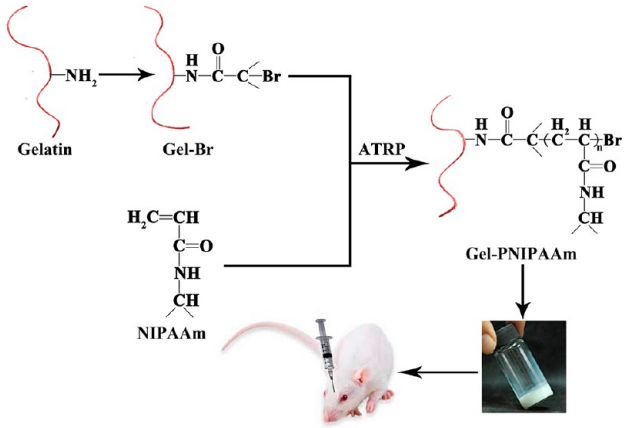

Figure 1. Schematic preparation of thermosensitive Gel−PNIPAAm hydrogel and its potential application for bone defect regeneration.

Compared to the coupling method, this approach was envisioned more controllable in adjusting the content and the length of the incorporated PNIPAAm due to the ATRP mechanism.[31] After the chemical structure being identified by characterizations as X-ray photoelectron spectroscopy (XPS), attenuated total reflection infrared spectroscopy (ATR-IR) and nuclear magnetic resonance (NMR), the potential of thermosensitive PNIPAAm-grafted gelatin (Gel−PNIPAAm) hydrogel for bone regeneration was evaluated by in vitro coculture with bone mesenchymal stem cells (BMSCs) and in vivo implantation in a cranial defect model. The effect of Gel−PNIPAAm/BMSCs construct on cranial defect regeneration was examined by histological, immunohistochemical and micro-CT analysis. The favorable hypothesis was that the injectable Gel−PNIPAAm hydrogel was able to serve as acceptable carrier for BMSCs and provide proper environment for orthopedic defect reconstruction.

EXPERIMENTAL SECTION

Materials. Gelatin (type B, from bovine, pH 4.5−5.5, bloom 240−270), α-bromoisobutyric acid (BIBA, 98%), *N*,*N*,*N*′,*N*′,*N*″-pentamethyl diethylenetriamine (PMDETA), copper(I) bromide (CuBr, 98%), 1-ethyl-3-(3-(dimethylamino)propyl) carbodiimide HCl (97%) (EDC), and *N*-hydroxysuccinimide (97%) (NHS) were purchased from Sigma-Aldrich Inc. (USA) and used directly. NIPAAm was obtained from Wako Pure Chemical Industry Ltd. (Osaka, Japan), and used after recrystallization from a toluene-hexane solution. All other chemicals used in producing Gel−PNIPAAm were of analytical pure grade, purchased from Beijing Chemical Plant (China), and used as received.

Preparation of Gel−PNIPAAm via ATRP. PNIPAAm was grafted onto gelatin via ATRP in two steps. Briefly, the ATRP macroinitiator (Gel−Br) was synthesized by reacting gelatin with BIBA using coupling agents (EDC/NHS) in reference to literature.[32] The grafting polymerization of NIPAAm was initiated by mixing Gel−Br, NIPAAm, PMDETA, and CuBr in dimethyl sulfoxide, and reacting at 30 °C under the protection of nitrogen gas.[33,34] At the end of the reaction, CuBr was removed by eluting the mixture solution through a column containing Al_2O_3, followed by dripping into ethanol to get the precipitation. The raw product was dissolved in DI water and dialyzed (MWCO of 50 000) with refreshed DI water at room temperature to obtain the purified Gel−PNIPAAm. Then it was freeze-dried and stored at 4 °C for further use.

Characterizations of Gel−PNIPAAm. Chemical composition of Gel−PNIPAAm was determined by XPS, ATR-IR, and NMR. XPS data were obtained using an AXIS Ultra instrument from Thermo V6 ESCALAB 25 (ThermoFisher Scientific, USA). ATR-IR spectra were recorded in the range of 400−4000 cm^{-1} with a resolution of 4 cm^{-1} on a Nicolet NEXUS-8700 FT-IR spectrometer (Madison, WI, USA). ^1H NMR spectra were recorded using a Bruker AV-400 spectrometer (Germany). The thermo-transition behavior of Gel−PNIPAAm was determined by measuring the light transmittance of Gel−PNIPAAm aqueous solution (5 mg/mL) along with increasing temperature in the range of 25−45 °C on a ultraviolet−visible spectrophotometer (UV-2600, UNICO, USA). At each temperature point, the solution was incubated at least 10 min before data recording. The measuring wavelength was set 350 nm.

In Vitro Cell Culture. Rat BMSCs (purchased from Cell Culture Center, Peking Union Medical College, China) were cultured in Dulbecco's modified Eagle's medium (DMEM, Hyclone) supplemented with 10% fetal bovine serum (FBS, PAA, Germany), 100 IU/mL penicillin (Sigma), and 100 mg/mL streptomycin (Sigma). The culture was maintained with 5% CO_2 at 37 °C and saturated humidity until 80% confluence prior to use.

The possible cytotoxicity of Gel−PNIPAAm hydrogel against BMSCs was evaluated in vitro. For this purpose, the cells were seeded in 96-well plates at 5×10^6 cells per well and incubated for 6 h. The culture medium was then removed and Gel−PNIPAAm solution in DMEM at concentration of 2 wt % was added. The cells were subjected to fluorescent staining analysis after being incubated for designated times (1, 3, 5, and 7 days). Attachment and survival of cells in the hydrogel solution was determined using fluorescent microscope (LW200-37XY, OLYMPUS) by live/dead staining with AO/EB. Cell proliferation was analyzed by nucleus staining with fluorescent Hochest 33528 and Cell Counting Kit-8 (CCK-8, Beyotime, China). At different culture time points (1, 3, 5, and 7 days), 20 μL of CCK-8 was added to each well and incubated at 37 °C in 5% CO_2 for 4 h. Then the OD values of liquid in each well were measured by a microreader (Biorad 580, USA) at the wavelength of 490 nm. The cell number was proportional to the OD value. BMSCs cultured in normal DMEM were applied as the control.

To reveal the cell growth within 3D hydrogel, Gel−PNIPAAm solution in DMEM at concentration of 10 wt % was used and BMSCs were mixed into the solution at room temperature. Gelation occurred as the temperature being raised to 37 °C. The system was maintained with 5% CO_2 at 37 °C and saturated humidity for 1, 3, 5, and 7 days. Photographs were taken by optical microscope (CKX31, OLYMPUS). Cell proliferation was determined by CCK-8 as aforedescribed.

Cranial Defect Regeneration. Two-week-old male SD rats were used in this animal experiment and randomly divided into three groups with four rats in each group. The experimental protocol was approved by the Animal Care and Use Committee of Tianjin Medical University, China.

The experimental calvarium defect was created by surgical procedure as follow. Rats were anesthetized with chloral hydrate (0.5 mL/250 kg). After shaving the skin and disinfecting the surgical site in each animal, a parallel skin incision was made in the middle of the calvarium. While exposing the bone tissue, a slowly rotating

DOI: 10.1021/acsami.5b02821
ACS Appl. Mater. Interfaces 2015, 7, 19006−19015

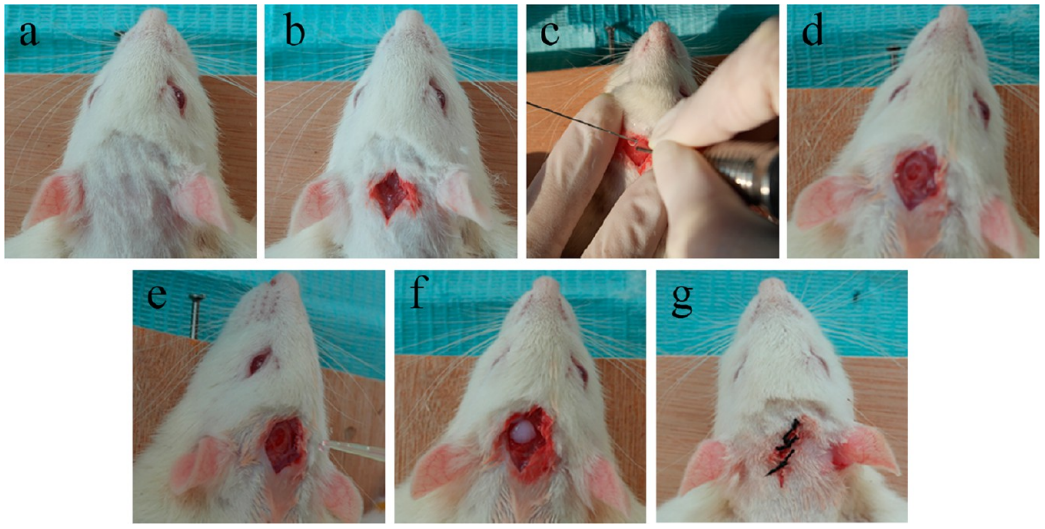

Figure 2. Operating procedure: (A) shaving the skin; (B) making skin incision; (C) creating circular defects; (D) appearance of the defect site; (E) injecting Gel−PNIPAAm solution; (F) hydrogel formation; (G) suturing the incision.

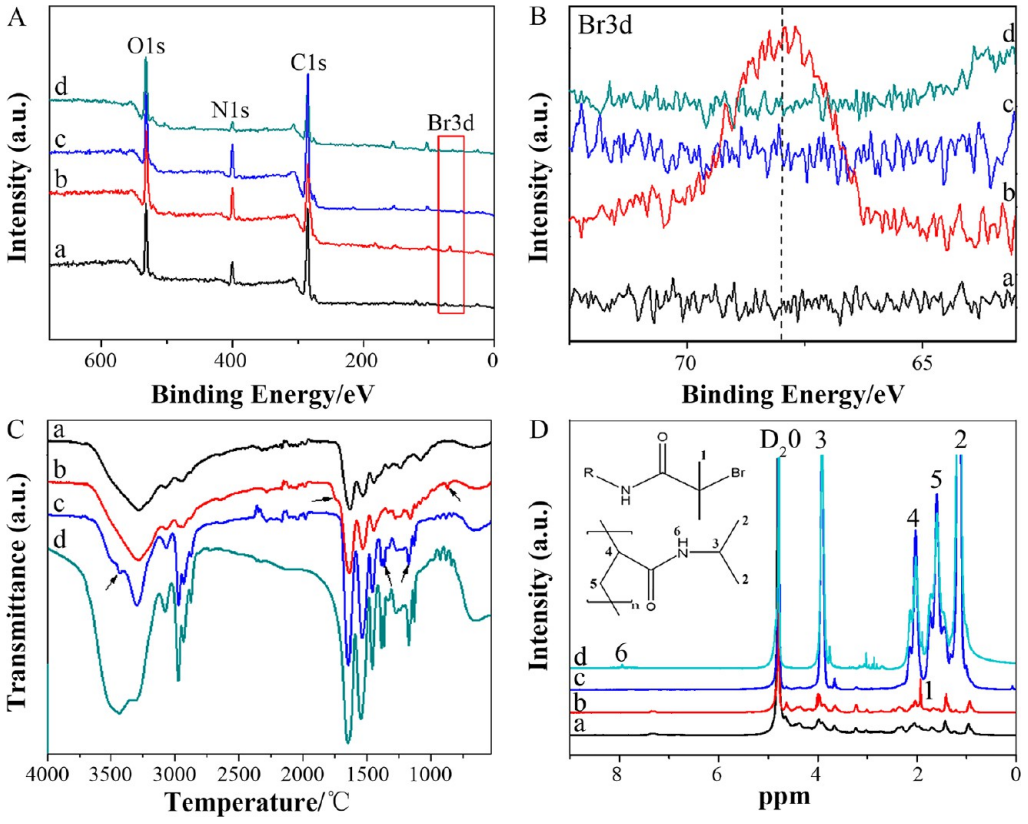

Figure 3. Characterizations of synthesized Gel−PNIPAAm by (A, B) XPS, (C) IR, and (D) ^{1}H NMR spectra: (a) pure gelatin, (b) Gel−Br, (c) Gel−PNIPAAm, and (d) pure PNIPAAm.

trephine burr was used to create circular defects with diameter about 5 mm under continuous saline irrigation in the left region on each rat. One group of rats was injected with Gel−PNIPAAm solution in DMEM (10%) into the defect. One group of rats was injected with Gel−PNIPAAm solution containing BMSCs (1×10^6 cells/ml). And one group of rats was left empty as control. After the injection, the solutions were observed transforming into hydrogels after standing for 30 s. Then the skin was carefully sutured over the defect area using absorbable suture (Figure 2). All the rats were allowed for free movement, as well as food and water uptake. Two rats from each group were sacrificed at 4 and 12 weeks postoperation.

Micro-CT Analysis. At weeks 4 and 12 after the surgery, calvarias were explanted from the three groups of rats, and fixed in 10% neutral buffered formalin for over 12 h. Then the harvested calvarias were scanned with Micro-CT scanner (Skyscan 1174, Aartselaar, Belgium). After the scans were completed, three-dimensional images of calvarium were reconstructed from the scans by the micro-CT system software package. CTAn software version 1.14 (Bruker micro-CT, Kontich, Belgium) was applied for the 3D morphological analysis of the micro-CT data. A cylindrical region of interest (ROI, 5 mm × 1 mm) was cocentrically positioned over the defect site. The parameters of bone volume fraction (bone volume/total volume, BV/TV) were used for

DOI: 10.1021/acsami.5b02821
ACS Appl. Mater. Interfaces 2015, 7, 19006−19015

comparison in this study. Defects for each group were measured at both 4 and 12 weeks and total volume of bone was reported (mm^3).

Histological and Immunohistochemical Staining. All the harvested calvarias were decalcified in a rapid decalcifier (RapidCal.Immuno, ZS-Bio, China) for 4 h at room temperature. Subsequently, the tissue samples were dehydrated and embedded in paraffin. Sections near the central area of the calvarium defect were used for histological/histomorphometrical and immunohistological analysis. The histological slices were stained by hematoxylin and eosin. To observe type I collagen, Masson staining was performed. The histological slices were deparaffinized and hydrated with distilled water. The hydrated slices were stained by Masson staining kit (Senbeijia, China) following the instruction of the manufacturer. Images were captured with optical microscope (CKX41, Olympus, Japan).

For immunostaining, endogenous peroxidase was blocked by incubating the sections with 3% hydrogen peroxide (H_2O_2). After washing the sections with phosphate buffer saline (PBS, pH 7.4, 0.01M), they were treated with 10% horse serum for 10 min to prevent nonspecific binding. Two osteogenic marker proteins, osteocalcin (OCN) and osteopontin (OPN), were detected by anti-OCN (Abcam, UK, cat. no. ab13420) and anti-OPN (Abcam, UK, cat. no. ab8448) primary antibody in 1:500 diluted solution with an antibody diluent (ZSGB-BIO, China), followed by incubation overnight at 4 °C. Thereafter, sections were rinsed three times with PBS for 5 min each and labeled using Polink-1 HRP DAB Detection System (GBI, USA), and incubated for 30 min in a moist chamber. Antibody complexes were visualized with 3,3-diaminobenzidine (DAB kit) as chromogen (ZSGB-BIO, China). As control, sections were parallel treated in a similar way without the incubation step of using the primary antibodies. The sections were dehydrated in ethanol and xylene and mounted using permanent medium. Stained sections were photographed using optical microscope. OCN and OPN expression within the defect area was quantified using Image Pro Plus 6.0 (IPP), a digitalized immunohistochemistry scoring program.[35,36]

Statistical Analysis. All quantitative data were expressed as mean ± standard deviation (SD) for n = 3. Statistical analysis was performed using the SPSS 19.0 software (Chicago, IL). Statistical difference was determined using Student's *t* test for independent samples. Differences between groups of $*p < 0.05$ were considered statistically significant and $**p < 0.01$ was considered highly significant.

RESULTS AND DISCUSION

Gel−PNIPAAm and Hydrogel Preparation. To graft PNIPAAm onto gelatin via ATRP, Gel−Br was synthesized as the macromolecular initiator in the first step. In comparison with pure gelatin, as shown in XPS spectra (Figure 3A and 3B), an extra signal was detected at 68 eV, which was assigned to the presence of Br_{3d}. Accordingly, a newly appearing peak at ~850 cm^{-1} was found in FT-IR spectrum of Gel−Br compared to that of pure Gel (Figure 3C). It was ascribed to the stretching vibration of C−Br. Additionally, the reaction of gelatin with BIBA would introduce new amide group into the molecular structure (Figure 1). Therefore, in addition to those characteristic absorption bands at 1650 cm^{-1} (amide I, C═O stretching), 1541 cm^{-1} (amide II, N−H bending) and 1238 cm^{-1} (amide III, N−H bending) resulting from pure gelatin, the extra small peak at 1760 cm^{-1} in the IR spectrum of Gel−Br further confirmed the successful synthesis of Gel−Br. In comparing the ^1H NMR spectra of pure gelatin and Gel−Br (Figure 3D), more solid proofs were found, that the appearance of a peak at 1.96 ppm (peak 1) was noted to the methyl group of BIBA in the sample of Gel−Br (Figure 3D, curve b). Different contents of BIBA could be introduced onto gelatin chains by adjusting the feeding ratio of BIBA to the free amino group in gelatin (see Figure S1 and Table S1).

The obtained Gel−Br was then used to initiate the polymerization of NIPAAm. After the reaction, it could be seen the disappearance of Br_{3d} signal in XPS spectrum of Gel−PNIPAAm (Figure 3A and 3B). In comparison with the FR-IR spectrum of PNIPAAm, the IR spectrum of Gel−PNIPAAm clearly displayed the existence of NIPAAm component (Figure 3C). The peaks between 1175 and 1155 cm^{-1} were ascribed to the stretching vibration of C−H of isopropyl group. The peaks at 1385 and 1365 cm^{-1} were the characteristic deformation vibration peaks of the methyl group in isopropyl group. Meanwhile, the stretching vibration of N−H between 3550 and 3420 cm^{-1} appeared. In the ^1H NMR spectra of Gel−PNIPAAm and pure PNIPAAm (Figure 3D, curve c and d), accordingly, peaks (peak 2−6, 1.15, 1.6, 2.0, 3.9, and 8.01 ppm) relating to different protons of NIPAAm component were clearly identified, as the molecular structure shown. In a word, PNIPAAm was successfully grafted onto gelatin using the aforementioned ATRP method.

Using Gel−Br with different contents of bromide element and changing the feeding ratios of NIPAAm monomer to gelatin, Gel−PNIPAAm copolymers with different contents and/or lengthes of PNIPAAm side chains could be obtained (see Table S2). The copolymers demonstrated different LCSTs (see Figure S2), and thus displayed different thermosensitive gelation potentials (See Figure S3). The Gel−PNIPAAm-2, which showed sharp sol-to-gel transition, was chosen for the following evaluations and referred as Gel−PNIPAAm.

Gel−PNIPAAm was dissolved in DI water, and the aqueous solution was submitted to transmittance measurement along temperature using pure PNIPAAm aqueous solution as reference. As shown in Figure 4, both PNIPAAm and Gel−PNIPAAm solutions displayed sharp decrease in transmittance as the temperature increasing. The LCST of PNIPAAm was detected ~32 °C as reported,[21,37] in which, the transparent PNIPAAm aqueous solution became cloudy when the temperature was above 32 °C. The phase transition of Gel−PNIPAAm took place at a higher temperature (~35 °C) than PNIPAAm. The increased LCST was resulting from the incorporation of hydrophilic gelatin component, because the phase transition of PNIPAAm was a kind of hydrophilic−hydrophobic transition. As the phase transition took place, the flowable Gel−PNIPAAm solution rapidly transformed into a hydrogel state from the gross morphological observation. Although the LCST of Gel−PNIPAAm was only 2 degrees lower than body temperature, the gelation could occur quickly when the Gel−

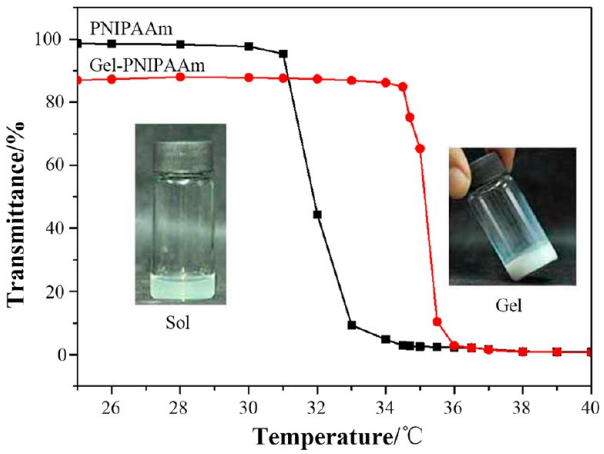

Figure 4. Phase transition analysis of the Gel−PNIPAAm aqueous solution (5 mg/mL) using a UV−vis spectrophotometry at 350 nm.

DOI: 10.1021/acsami.5b02821
ACS Appl. Mater. Interfaces 2015, 7, 19006−19015

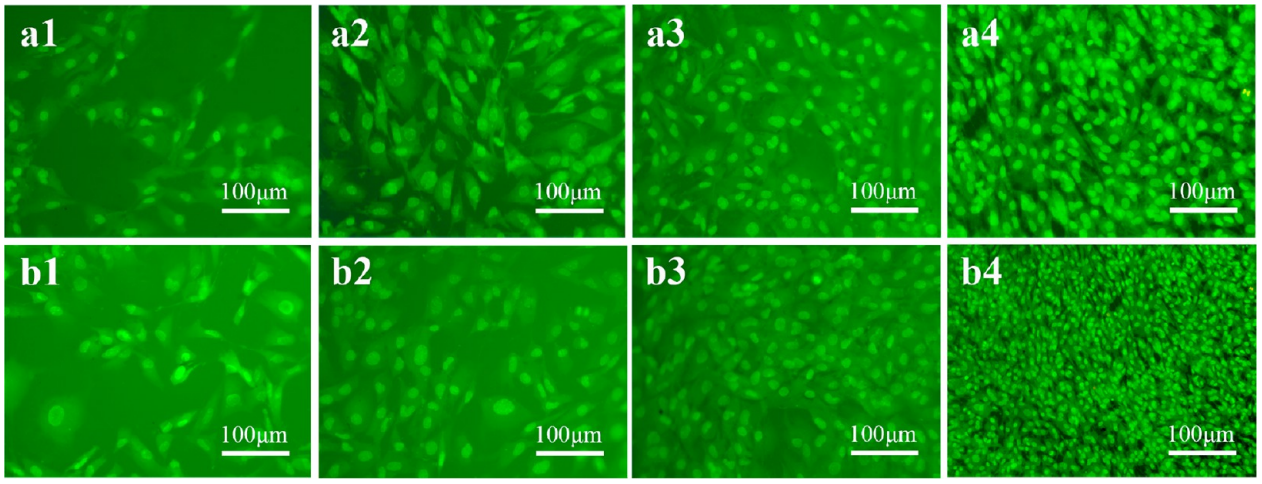

Figure 5. Live/dead assay of BMSCs proliferated in normal DMEM (upper row) and Gel−PNIPAAm/DMEM solution (2 wt %, lower row) for 1 (a1, b1), 3 (a2, b2), 5 (a3, b3), and 7 days (a4, b4) by AO/EB staining (green, live; red, dead).

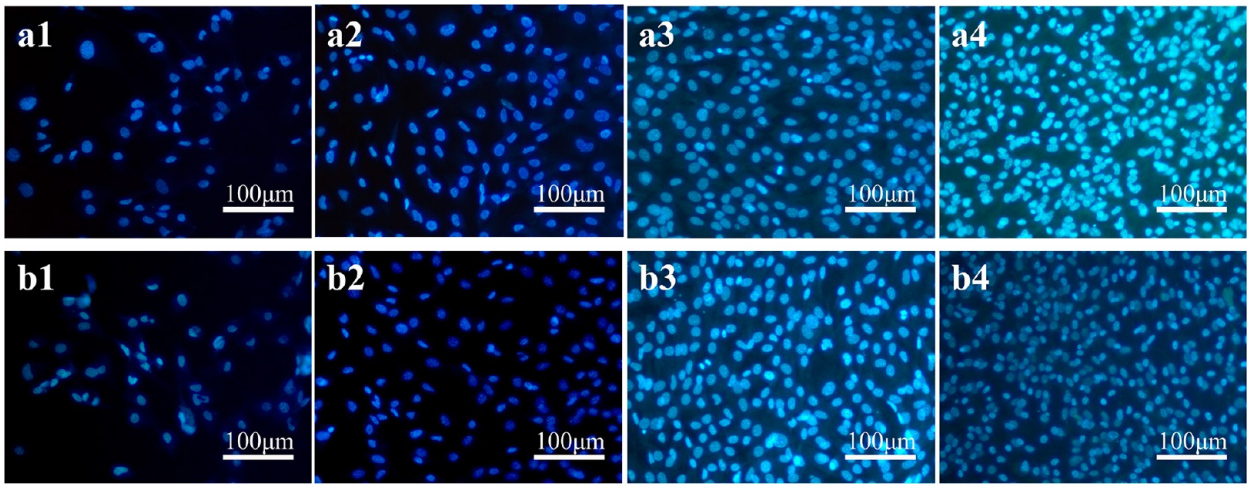

Figure 6. Fluorescent images of BMSCs stained by Hoechst 33528 showing the morphology of cell nuclei and the proliferation of BMSCs cultured in normal DMEM (upper row) and Gel−PNIPAAm/DMEM solution (2 wt %, lower row) for 1 (a1, b1), 3 (a2, b2), 5 (a3, b3), and 7 days (a4, b4).

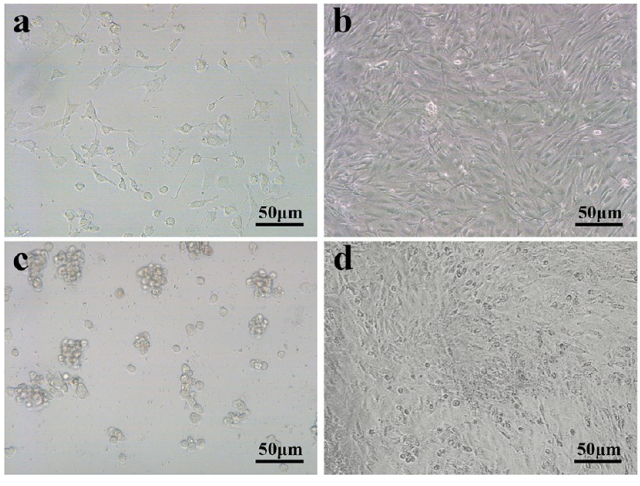

Figure 7. Optical micrographs showing cell morphologies after BMSCs being cultured in different Gel−PNIPAAm/DMEM solutions for 1 day and 5 days: (a) 2 wt %, 1 day; (b) 2 wt %, 5 days; (c) 10 wt %, 1 day; (d) 10 wt %, 5 days.

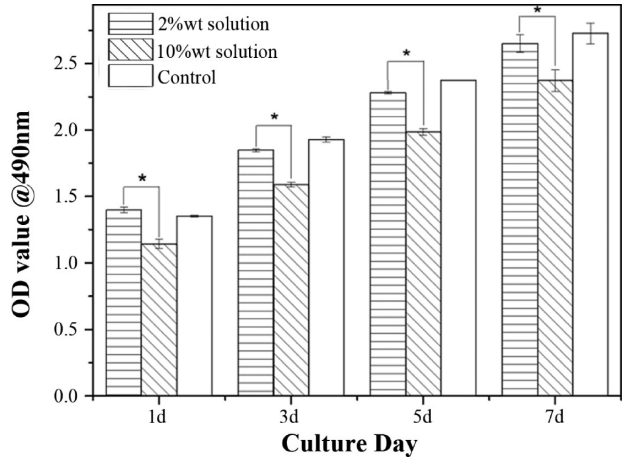

Figure 8. Cell proliferation in vitro in the presence of Gel−PNIPAAm solutions of different concentrations that 2 wt % solution was in liquid state and 10 wt % solution was in a hydrogel state.

PNIPAAm solution were dropped into warm water thermoset at 37 °C. Therefore, Gel−PNIPAAm aqueous solution was

DOI: 10.1021/acsami.5b02821
ACS Appl. Mater. Interfaces 2015, 7, 19006−19015

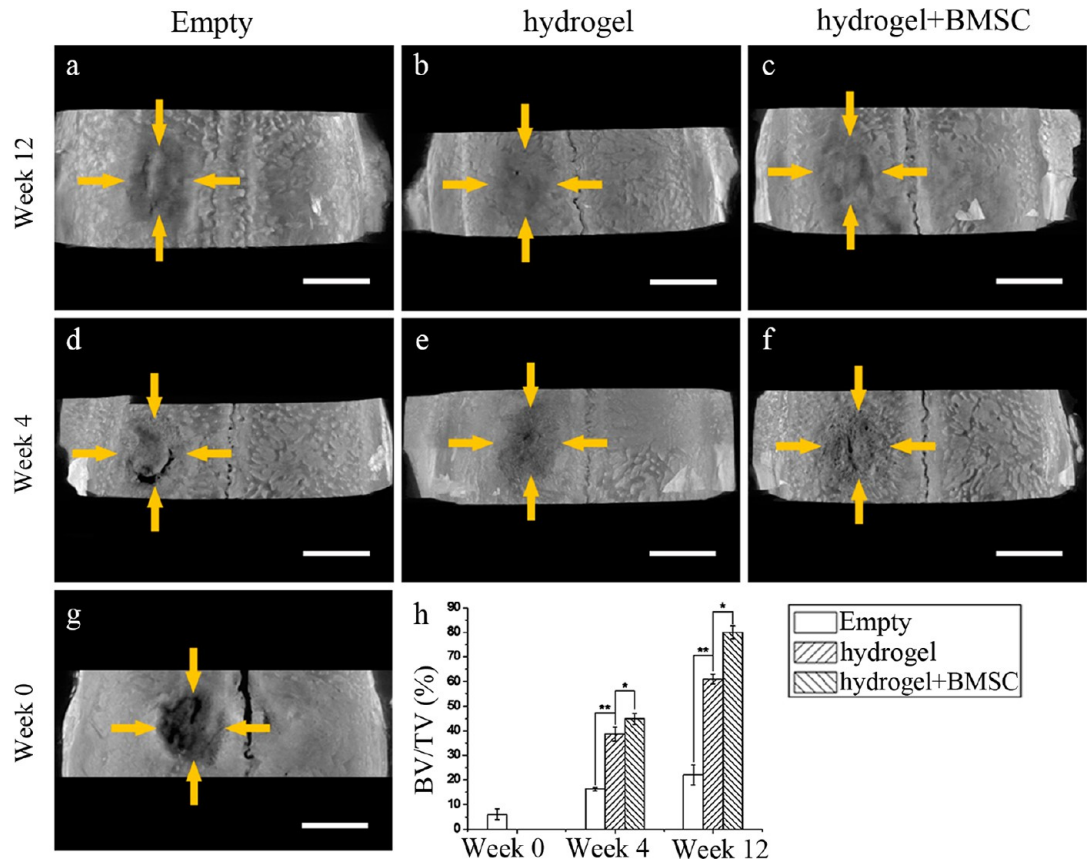

Figure 9. Representative 3D micro-CT photographs of rat cranial bone defects (a–g) and quantitative analysis of the ratios of the bone volume/total volume (BV/TV ratio) (h) at 4 and 12 weeks postimplantation. Arrows indicate the edges of host bone. Scale bar: 5 mm. (*p < 0.05 and **p < 0.01).

envisioned possible carrier for BMSCs as injective thermosensitive hydrogel material.

Cytotoxicity Evaluation of Gel–PNIPAAm Hydrogel in Vitro. In preparation of Gel–PNIPAAm by ATRP, reagents as NIPAAm monomer, PMDETA and CuBr catalysts were used. The resulting Gel–PNIPAAm might have some cytotoxicity if these compounds were not purified completely. In vitro coculture of rat BMSCs with Gel–PNIPAAm/DMEM solution was then carried out to determine its cytotoxicity. For the purpose to avoid the loss of cells in seeding, in the culture, the Gel–PNIPAAm/DMEM solution (2 wt %) was gently dropped into the wells after the cell suspension had been added into culture plate and incubated for 6 h allowing for cell adhesion. BMSCs were observed attaching onto tissue culture polystyrene plate gradually and proliferated continuously in both the control group and the Gel–PNIPAAm group under optical microscope observation. At 1, 3, 5, and 7 days after cell seeding, live/dead assay was performed by AO/EB staining. As shown in Figure 5, cell numbers could be seen clearly increasing with longer culture time and comparable in both cases. The cells were in normal spindle-like shape and mostly stained green. Red staining spot could be hardly found at all time points. BMSCs viability in the 3D Gel–PNIPAAm hydrogel was also evaluated by using live/dead staining (see Figure S4). Live cells stained green had been detected at all time points, along with a gradually increase in cell number with longer culture time, which clearly indicated the cell viability within the gel.

BMSCs proliferation was first evaluated by nuclei staining with Hoechst and optical microscope observation. Those fluorescent images in Figure 6 illustrated and confirmed that BMSCs grew continuously in both DMEM solution and Gel–PNIPAAm/DMEM solution (2 wt %) with culture time, showing normal morphology of cell nuclei and similar in both cases. However, the BMSCs embedded in the Gel–PNIPAAm hydrogel (10 wt % Gel–PNIPAAm solution in DMEM) displayed cell spreading behavior different from those in Gel–PNIPAAm/DMEM solution (2 wt %). As shown in Figure 7, BMSCs had spread into spindal shape on TCPS after 1 day culture (Figure 7a), and grown into confluent state after 5 days culture (Figure 7b), as the 2 wt % Gel–PNIPAAm/DMEM solution was used as the culture medium. In the case of 3D hydrogel culture, the embedded BMSCs mainly remained spherical shape and did not spread at the first day of culture (Figure 7c). To the fifth day of culture, however, most of the cells were detected having spread into spindal shape (Figure 7d), which revealed that cell viability was still quite good in the 3D hydrogel.

The proliferation of BMSCs in different culture conditions were quantitatively analyzed and compared using CCK-8. As shown in Figure 8, BMSCs were able to proliferate continuously in all the three cases. It was found that the cell growth rate in 2 wt % Gel–PNIPAAm/DMEM solution was comparable to that in the control group, showing no significant difference. The result distinctly suggested the Gel–PNIPAAm material had no obvious cytotoxicity to BMSCs. While the cell proliferation in the 3D hydrogel situation was a little inferior to others for all the time points. Together with the cell morphological observations shown in Figure 7, one of the

DOI: 10.1021/acsami.5b02821
ACS Appl. Mater. Interfaces 2015, 7, 19006–19015

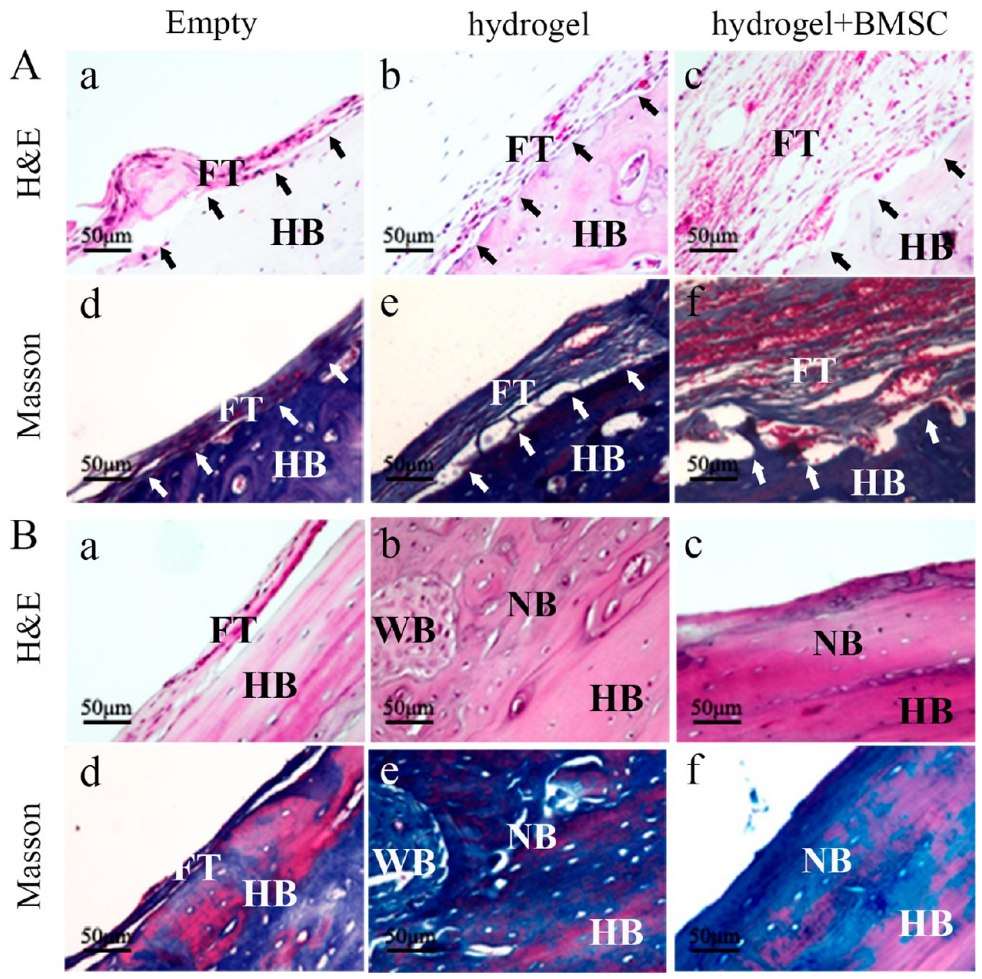

Figure 10. Histological analysis of bone formation at 4 (A) and 12 weeks (B) postimplantation by H&E staining (a–c) and Masson's trichrome staining (d–f). Arrows denote the boundary between new bone and host bone (HB, host bone; NB, new bone; WB, woven bone; FT, fibrous tissue). Scale bar 50 μm.

possible explanation for this point was the slower spreading rate of BMSCs in the 3D hydrogel environment, which had slowed the cell growth.[38,39] Another possible reason might be the reduced mass transfer rate within the gel having impeded the cell growth compared with other two cases.[40,41] However, the continuous proliferation of BMSCs detected in the 3D Gel–PNIPAAm hydrogel displayed that the hydrogel could be used as BMSCs carrier for in vivo bone regeneration.

Cranial Defect Regeneration. Thermosensitive Gel–PNIPAAm had the advantage as injectable hydrogel material for defect regeneration. Instead of soft tissue regeneration, in this study, critical bone defect protocol (5 mm-sized) was created using cranial model to evaluate the potential of using injectable hydrogel for hard tissue reparation. As illustrated in Figure 2, Gel–PNIPAAm/DMEM solution of 10 wt % containing BMSCs or not was injected into the circular defect on rat calvarium. After standing for 30 s, gelation took place and the solution could not flow anymore. At 4 and 12 weeks after calvarial implantation, rats were euthanized and defect sites were harvested to evaluate bone regeneration using untreated blank defect as control.

At first, micro-CT images were taken to assess the 3D structure of the repaired skull, and the images are shown in Figure 9. Obviously, the contour of the defect could be easily identified in the control group 12 weeks postoperation, indicating nonhealing of the critical-sized defect within the experimental period. While in both the hydrogel and hydrogel/BMSCs filling groups, the boundary between the cranial defect site and surrounding host bone was already indistinct after 12 weeks of the implantation, and substantial new bone formation was observed. From 4 weeks to 12 weeks, the bone regeneration rate seemed even faster in the hydrogel/BMSCs group than that in the hydrogel group from the images. The surface morphology of the healed defects closely resembled that of the surrounding normal bone. To quantitatively understand the situation, bone volume fraction (i.e., bone volume/total volume, BV/TV) was assessed by morphometric analysis and compared in Figure 9h. The BV/TV data could be seen increasing gradually in all cases, but in different increasing rates. The highest value was displayed by the hydrogel/BMSCs group, followed by the hydrogel group and the control group.

The decalcified tissue sections were then histological analyzed by both H&E and Masson's Trichrome staining. At 4 weeks postoperation, as shown in Figure 10A, the boundary between the defect area and the host bone was clearly identified (marked by black arrows) in all the three groups. The H&E staining displayed the bone defect areas were covered with fibrous connective tissues. And the new filling tissue in the defect area demonstrated different thickness in the order of hydrogel/BMSCs group > hydrogel group > control group.

DOI: 10.1021/acsami.5b02821
ACS Appl. Mater. Interfaces 2015, 7, 19006–19015

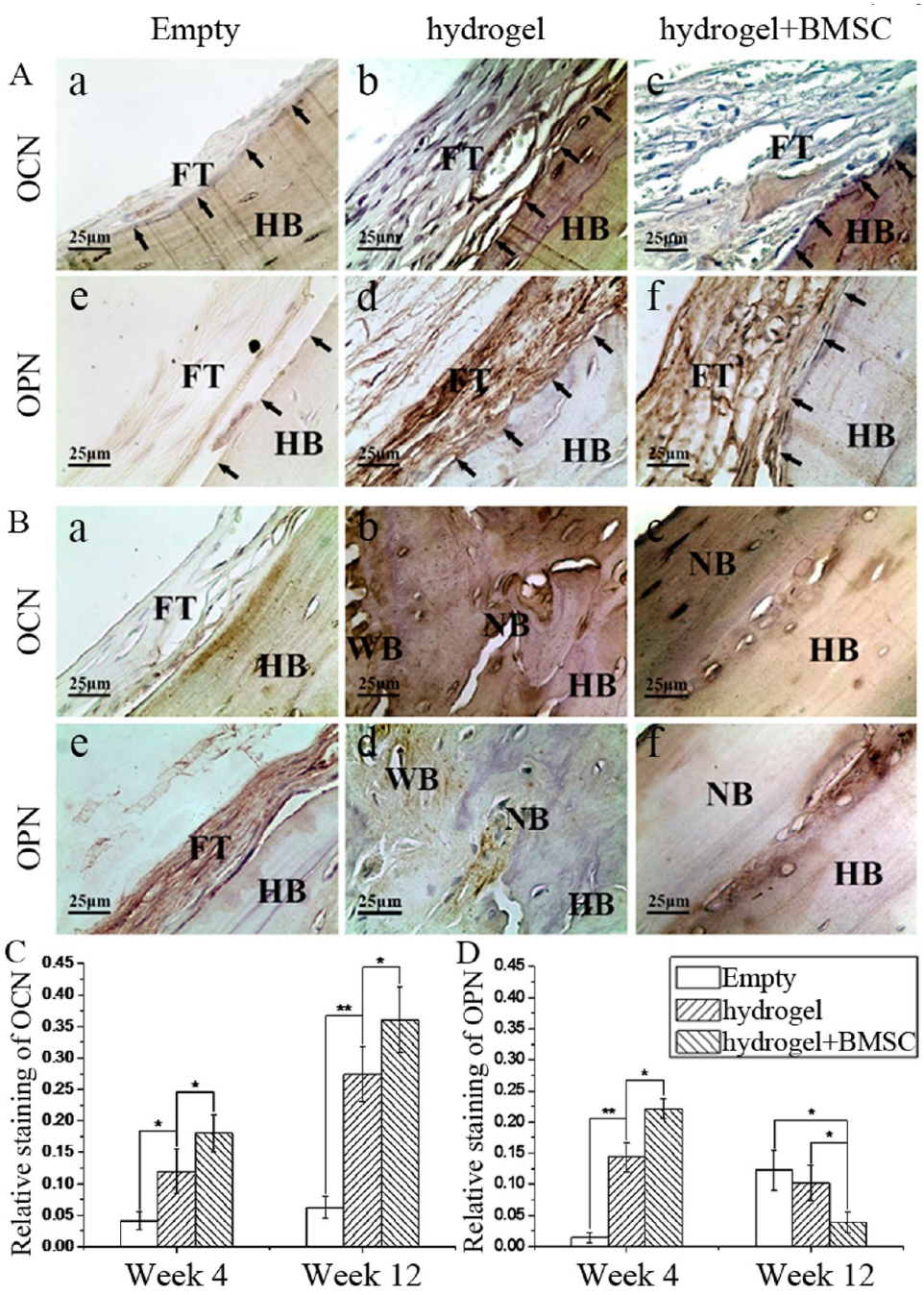

Figure 11. Immunohistochemical staining of cranial defect sections for OCN (a–c) and OPN (d–f) expression at 4 (A) and 12 (B) weeks postimplantation, together with the staining intensities of OCN (C) and OPN (D). Black arrows denote the boundary between new bone and host bone (HB, host bone; NB, new bone; WB, woven bone; FT, fibrous tissue). Scale bar: 25 μm. (*p < 0.05 and **p < 0.01).

Masson's Trichrome staining confirmed that the untreated defect was filled with fibrous tissue (Figure 10A(d)), while, the staining revealed that those fibrous tissues in both hydrogel and hydrogel/BMSCs groups were mainly composed of collagen fibers (Figure 10A(e and f), indicating the newly formed periosteum. The incorporation of BMSCs into the Gel–PNIPAAm hydrogel apparently enhanced the regeneration process from the early stage. Up to 12 weeks postoperation, a dense layer composed of fibrous tissue was distinctly observed in the control group with little evidence of spontaneous bone regeneration, confirming the formation of connective tissues in untreated bone defect (Figure 10B(a and d)). In the hydrogel group, numerous newly formed osteoid tissue and woven bone with rich collagen expression was easily identified, and interface between the nascent bone and the host bone was still distinguishable (Figure 10B(b and e)). For the hydrogel/BMSCs group, however, the defects had been filled with calcified lamellar bone, which connected to the surrounding mature host bone firmly with indistinguishable boundary at 12 weeks postoperation (Figure 10B(c and f)). Both the H&E and Masson's Trichrome staining results declared the successful bone defect healing with Gel–PNIPAAm hydrogel/BMSCs treatment.

As new bone formation should be accompanied by the expression of proteins that marked the osteogenic progression, immunohistochemical analysis was evaluated qualitatively and

DOI: 10.1021/acsami.5b02821
ACS Appl. Mater. Interfaces 2015, 7, 19006–19015

quantitatively from sections of the defects (Figure 11). In the untreated group at both 4 and 12 weeks postoperation (Figure 11A(a) and Figure 11B(a)), the high magnification images of host bone and regions adjacent to the defect sites demonstrated rarely expression of OCN, a specific marker of osteogenic differentiation and mineralization. On the contrary, intense staining of OCN was observed in both the hydrogel group and the hydrogel/BMSCs group at both 4 and 12 weeks (Figure 11A and Figure 11B). The expression of OCN increased with longer implantation time. Of interest, the OCN staining demonstrated significantly greater intensity at both time points in the hydrogel/BMSCs group (Figure 11C). Among the three groups, OCN was most prevalent in the hydrogel/BMSCs group all the time. A little bit differently, the expression of OPN, another marker of bone maturation, displayed the highest intensity in the hydrogel/BMSCs group at 4 weeks, and subsequently decreased to the lowest at longer implantation time of 12 weeks (Figure 11D). In comparing the Figure 11B(e) and Figure 11B(f), positively stained OPN expression could be seen more apparent in woven bone than in the lamellar bone, that is, the newly formed bone tissue likely showed an increased expression of OPN.

All the aforementioned results demonstrated the fact that thermosensitive Gel−PNIPAAm hydrogel was biocompatible and good substrate to induce in vivo bone defect regeneration in combination with BMSCs. Gelatin, a denatured collagen, was a good substrate for tissue engineering itself, but cross-linking was normally required for the practical use. PNIPAAm, a negative thermosensitive polymer with LCST of ∼32 °C, became insoluble in aqueous solution above the LCST. Therefore, injectable Gel−PNIPAAm hydrogel was readily obtained by introducing PNIPAAm side chains onto gelatin backbone, in which, the hydrophobic transition of PNIPAAm side chains under body temperature would act as physical cross-linking joints for the gelatin backbone. When the Gel−PNIPAAm hydrogel was used to fill the rat cranial defect, new bone formation was able to be detected along with time in comparison with the untreated defect. Fibrous tissue had grown into the defect area in the control group, while woven bone tissue formed in the hydrogel-treated group with relatively high expression of OCN and OPN. The outcomes revealed the feasibility of using injective thermosensitive Gel−PNIPAAm hydrogel to repair bone defect. The bone regeneration rate could be significantly enhanced by incorporating BMSCs into the Gel−PNIPAAm hydrogel. At 12 weeks postimplantation, lamellar bone could be seen having formed and filled the defect area. The difference between the nascent bone tissue and the surrounding host bone tissue could be hardly told. Quantitatively, the regenerated bone tissue had reached the BV/TV value as high as ∼80% in the hydrogel/BMSCs group, which was significantly higher than those in other two groups. It was reasonably to summary that the thermosensitive Gel−PNIPAAm hydrogel was an excellent injectable delivery vehicle of BMSCs for in vivo bone defect regeneration.

CONCLUSIONS

Thermosensitive hydrogel deriving from negative thermosensitive PNIPAAm modified gelatin could be used as injectable repairing material to fill bone defect in vivo. ATRP was an easy and effective to synthesize gelatin-PNIPPAAm in comparison with conventional coupling method. Gelatin-PNIPPAAm aqueous solution displayed rapid sol-to-gel transition as the environmental temperature being increased above its LCST. The hydrogel demonstrated good biocompatibility, and behaved as excellent carrier for BMSCs to induce new bone formation in vivo. Bone healing was achieved with the in situ-formed Gel−PNIPAAm/BMSCs hydrogel complex in rat cranial defects.

ASSOCIATED CONTENT

Supporting Information

The Supporting Information is available free of charge on the ACS Publications website at DOI: 10.1021/acsami.5b02821.

Preparation and characterization of Gel−Br with different contents of bromine element, corresponding Gel−PNIPAAm copolymers synthesized by using the aforementioned Gel−Br as initiators, sol−gel transition of resulting Gel−PNIPAAm aqueous solutions, and live/dead assay on BMSCs viability in the 3D thermosensitive Gel−PNIPAAm hydrogel (PDF)

AUTHOR INFORMATION

Corresponding Authors

*E-mail: zhxden@126.com.

*E-mail: caiqing@mail.buct.edu.cn.

Notes

The authors declare no competing financial interest.

ACKNOWLEDGMENTS

All the authors received funding from National Basic Research Program of China (2012CB933904). Q.C. and S.D. received funding from National Natural Science Foundation of China (No. 51473016, 51472068). Q.C. and X.Y. received funding from Beijing Municipal Commission of Education (ZDZH20141001001).

REFERENCES

(1) Kretlow, J. D.; Mikos, A. G. Review: Mineralization of Synthetic Polymer Scaffolds for Bone Tissue Engineering. *Tissue Eng.* **2007**, *13*, 927−938.

(2) Stevens, B.; Yang, Y.; Mohandas, A.; Stucker, B.; Nguyen, K. T. A Review of Materials, Fabrication Methods, and Strategies Used to Enhance Bone Regeneration in Engineered Bone Tissues. *J. Biomed. Mater. Res., Part B* **2008**, *85*, 573−582.

(3) Tabata, Y. Tissue Regeneration Based on Tissue Engineering Technology. *Congenital Anomalies* **2004**, *44*, 111−124.

(4) Stevens, M. M.; George, J. H. Exploring and Engineering the Cell Surface Interface. *Science* **2005**, *310*, 1135−1138.

(5) Srouji, S.; Kizhner, T.; Livne, E. 3D Scaffolds for Bone Marrow Stem Cell Support in Bone Repair. *Regener. Med.* **2006**, *1*, 519−528.

(6) Srouji, S.; Kizhner, T.; Livne, E. Microscopy Analysis of Bone Marrow-derived Osteoprogenitor Cells Cultured on Hydrogel 3-D Scaffold. *Microsc. Res. Tech.* **2005**, *66*, 132−138.

(7) Barrilleaux, B.; Phinney, D. G.; Prockop, D. J.; O'Connor, K. C. Review: Ex Vivo Engineering of Living Tissues with Adult Stem Cells. *Tissue Eng.* **2006**, *12*, 3007−3019.

(8) Mai, R.; Hagedorn, M. G.; Gelinsky, M.; Werner, C.; Turhani, D.; Spath, H.; Gedrange, T.; Lauer, G. Ectopic Bone Formation in Nude Rats Using Human Osteoblasts Seeded Poly(3)hydroxybutyrate Embroidery and Hydroxyapatite-collagen Tapes Constructs. *J. Cranio. Maxill. Surg.* **2006**, *34*, 101−109.

(9) Dubruel, P.; Unger, R.; Van Vlierberghe, S.; Cnudde, V.; Jacobs, P. J. S.; Schacht, E.; Kirkpatrick, C. J. Porous Gelatin Hydrogels: 2. In Vitro Cell Interaction Study. *Biomacromolecules* **2007**, *8*, 338−344.

(10) Oh, S. H.; Kang, S. G.; Kim, E. S.; Cho, S. H.; Lee, J. H. Fabrication and Characterization of Hydrophilic Poly(Lactic-co-glycolic Acid)/Poly(Vinyl Alcohol) Blend Cell Scaffolds By Melt-

DOI: 10.1021/acsami.5b02821
ACS Appl. Mater. Interfaces 2015, 7, 19006−19015

Molding Particulate-Leaching Method. *Biomaterials* **2003**, *24*, 4011−4021.
(11) Hua, F. J.; Kim, G. E.; Lee, J. D.; Son, Y. K.; Lee, D. S. Macroporous Poly (L-lactide) Scaffold 1. Preparation of a Macroporous Scaffold By Liquid-liquid Phase Separation of a PLLA-dioxane-water System. *J. Biomed. Mater. Res.* **2002**, *63*, 161−167.
(12) Seitz, H.; Rieder, W.; Irsen, S.; Leukers, B.; Tille, C. Three-dimensional Printing of Porous Ceramic Scaffolds for Bone Tissue Engineering. *J. Biomed. Mater. Res., Part B* **2005**, *74*, 782−788.
(13) Ekenseair, A. K.; Kasper, F. K.; Mikos, A. G. Perspectives on the Interface of Drug Delivery and Tissue Engineering. *Adv. Drug Delivery Rev.* **2013**, *65*, 89−92.
(14) Tan, H.; Marra, K. G. Injectable, Biodegradable Hydrogels for Tissue Engineering Applications. *Materials* **2010**, *3*, 1746−1767.
(15) Seliktar, D. Designing Cell-compatible Hydrogels for Biomedical Applications. *Science* **2012**, *336*, 1124−1128.
(16) McKay, C. A.; Pomrenke, R. D.; McLane, J. S.; Schaub, N. J.; DeSimone, E. K.; Ligon, L. A.; Gilbert, R. J. An Injectable, Calcium Responsive Composite Hydrogel for the Treatment of Acute Spinal Cord Injury. *ACS Appl. Mater. Interfaces* **2014**, *6*, 1424−1438.
(17) Wu, J.; Su, Z. G.; Ma, G. H. A Thermo-and pH-Sensitive Hydrogel Composed of Quaternized Chitosan/Glycerophosphate. *Int. J. Pharm.* **2006**, *315*, 1−11.
(18) Amini, A. A.; Nair, L. S. Injectable Hydrogels for Bone and Cartilage Repair. *Biomed. Mater.* **2012**, *7*, 024105.
(19) Jeong, B.; Kim, S. W.; Bae, Y. H. Thermosensitive Sol-gel Reversible Hydrogels. *Adv. Drug Delivery Rev.* **2002**, *54*, 37−51.
(20) Tan, H.; Ramirez, C. M.; Miljkovic, N.; Li, H.; Rubin, J. P.; Marra, K. G. Thermosensitive Injectable Hyaluronic Acid Hydrogel for Adipose Tissue Engineering. *Biomaterials* **2009**, *30*, 6844−6853.
(21) Gao, J.; Wu, C. The "Coil-to-globule" Transition of Poly (N-isopropylacrylamide) on the Surface of a Surfactant-free Polystyrene Nanoparticle. *Macromolecules* **1997**, *30*, 6873−6876.
(22) Chen, J. P.; Cheng, T. H. Thermo-responsive Chitosan-graft-poly(N-sopropylacrylamide) Injectable Hydrogel for Cultivation of Chondrocytes and Meniscus Cells. *Macromol. Biosci.* **2006**, *6*, 1026−1039.
(23) Mu, Q.; Fang, Y. Preparation of Thermosensitive Chitosan with Poly (N-isopropylacrylamide) Side at Hydroxyl Group via O-maleoyl-N-phthaloyl-chitosan (MPCS). *Carbohydr. Polym.* **2008**, *72*, 308−314.
(24) Chen, J. P.; Lee, W. L. Collagen-grafted Temperature-Responsive Nonwoven Fabric for Wound Dressing. *Appl. Surf. Sci.* **2008**, *255*, 412−415.
(25) Ha, D. I.; Lee, S. B.; Chong, M. S.; Lee, Y. M.; Kim, S. Y.; Park, Y. H. Preparation of Thermo-responsive and Injectable Hydrogels Based on Hyaluronic Acid and Poly(N-isopropylacrylamide) and their Drug Release Behaviors. *Macromol. Res.* **2006**, *14*, 87−93.
(26) Varghese, J. M.; Ismail, Y. A.; Lee, C. K.; Shin, K. M.; Shin, M. K.; Kim, S. I.; So, I.; Kim, S. J. Thermoresponsive Hydrogels Based on Poly (N-isopropylacrylamide)/Chondroitin Sulfate. *Sens. Actuators, B* **2008**, *135*, 336−341.
(27) Ohya, S.; Kidoaki, S.; Matsuda, T. Poly (N-isopropylacrylamide) (PNIPAM)-grafted Gelatin Hydrogel Surfaces: Interrelationship between Microscopic Structure and Mechanical Property of Surface Regions and Cell Adhesiveness. *Biomaterials* **2005**, *26*, 3105−3111.
(28) Tan, H.; Chu, C. R.; Payne, K. A.; Marra, K. G. Injectable in Situ Forming Biodegradable Chitosan−hyaluronic Acid Based Hydrogels for Cartilage Tissue Engineering. *Biomaterials* **2009**, *30*, 2499−2506.
(29) Lai, J. Y.; Hsieh, A. C. A Gelatin-g-poly(N-isopropylacrylamide) Biodegradable in Situ Gelling Delivery System for the Intracameral Administration of Pilocarpine. *Biomaterials* **2012**, *33*, 2372−2387.
(30) Wu, D. Q.; Qiu, F.; Wang, T.; Jiang, X. J.; Zhang, X. Z.; Zhuo, R. X. Toward the Development of Partially Biodegradable and Injectable Thermoresponsive Hydrogels for Potential Biomedical Applications. *ACS Appl. Mater. Interfaces* **2009**, *1*, 319−327.
(31) Matyjaszewski, K. Atom Transfer Radical Polymerization (ATRP): Current Status and Future Perspectives. *Macromolecules* **2012**, *45*, 4015−4039.
(32) Yan, P.; Zhao, N.; Hu, H.; Lin, X.; Liu, F.; Xu, F. A Facile Strategy to Functionalize Gold Nanorods with Polycation Brushes for Biomedical Applications. *Acta Biomater.* **2014**, *10*, 3786−3794.
(33) Xu, F. J.; Zheng, Y. Q.; Zhen, W. J.; Yang, W. T. Thermoresponsive Poly (N-isopropyl Acrylamide)-grafted Polycaprolactone Films with Surface Immobilization of Collagen. *Colloids Surf., B* **2011**, *85*, 40−47.
(34) Hu, Y.; Zhao, N. N.; Li, J. S.; Yang, W. T.; Xu, F. J. Temperature-responsive Porous Polycaprolactone-based Films via Surface-initiated ATRP for Protein Delivery. *J. Mater. Chem.* **2012**, *22*, 21257−21264.
(35) Krueckl, S. L.; Sikes, R. A.; Edlund, N. M.; Bell, R. H.; Coll, A. H.; Fazli, L.; Gleave, M. E.; Cox, M. E. Increased Insulin-like Growth Factor I Receptor Expression and Signaling are Components of Androgen-independent Progression in a Lineage-derived Prostate Cancer Progression Model. *Cancer Res.* **2004**, *64*, 8620−8629.
(36) Wang, C. J.; Zhou, Z. G.; Holmqvist, A.; Zhang, H.; Li, Y.; Adell, G.; Sun, X. F. Survivin Expression Quantified by Image Pro-plus Compared with Visual Assessment. *Appl. Immunohistochem. Mol. Morphol.* **2009**, *17*, 530−535.
(37) Brazel, C. S.; Peppas, N. A. Synthesis and Characterization of Thermo- and Chemomechanically Responsive Poly (N-isopropylacrylamide-co-methacrylic Acid) Hydrogels. *Macromolecules* **1995**, *28*, 8016−8020.
(38) Chen, C. S.; Mrksich, M.; Huang, S.; Whitesides, G. M.; Ingber, D. E. Geometric Control of Cell Life and Death. *Science* **1997**, *276*, 1425−1428.
(39) Burdick, J. A.; Anseth, K. S. Photoencapsulation of Osteoblasts in Injectable RGD-Modified PEG Hydrogels for Bone Tissue Engineering. *Biomaterials* **2002**, *23*, 4315−4323.
(40) Hwang, C. M.; Sant, S.; Masaeli, M.; Kachouie, N. N.; Zamanian, B.; Lee, S.; Khademhosseini, A. Fabrication of Three-Dimensional Porous Cell-Laden Hydrogel for Tissue Engineering. *Biofabrication* **2010**, *2*, 035003.
(41) Ji, C.; Khademhosseini, A.; Dehghani, F. Enhancing Cell Penetration and Proliferation in Chitosan Hydrogels for Tissue Engineering Applications. *Biomaterials* **2011**, *32*, 9719−9729.

DOI: 10.1021/acsami.5b02821
ACS Appl. Mater. Interfaces 2015, 7, 19006−19015